

Modulation spectroscopy of the complex photoluminescence band of $\text{Ga}_{0.7}\text{Al}_{0.3}\text{As:Si}$

B. Gil,* M. Leroux, J. P. Contour, and C. Chaix†

Laboratoire de Physique des Solides et Energie Solaire, Rue Bernard Gregory, Sophia-Antipolis, 06560 Valbonne, France

(Received 10 December 1990)

The photoluminescence and reflectivity of $\text{Ga}_{0.7}\text{Al}_{0.3}\text{As:Si}$ have been studied in piezomodulation, wavelength-modulation, and photomodulation spectroscopy at low temperatures. We could identify the symmetry of the zero-phonon and phonon-assisted transitions by their comparative behavior in wavelength- and piezomodulated spectroscopy. The experimental results have been interpreted in the framework of an effective-mass model of the donor wave function in multivalley semiconductors similar to that proposed by Henning, Ansems, and Roksnoer [Semicond. Sci. Technol. **3**, 361 (1988)]. Within this model, a value of the hydrostatic deformation potential of the L band in this alloy is deduced: -4.99 ± 0.07 eV.

I. INTRODUCTION

It is nowadays well established that n -type impurities in $\text{Ga}_{1-x}\text{Al}_x\text{As}$ give, in addition to the effective-mass donor, a deep state, the DX center.¹ There is strong evidence that the shallow and the deep DX levels are, in fact, two possible configurations of the same impurity center.² The deep level exhibits bistability, an electron-capture cross section which is thermally activated. Although it is well established that the deep level is due to the dopant, a controversy concentrates on the magnitude of the lattice relaxation.³ This has given models based upon displacement of the substitutional donor with either large or small lattice relaxation. The line shape of the complex luminescence band of $\text{Ga}_{1-x}\text{Al}_x\text{As}$ has been intensively studied by Henning, Ansems, and Roksnoer,⁴ who revealed the existence of four donor levels in $\text{Ga}_{1-x}\text{Al}_x\text{As:Si}$. By studying the alloy composition dependence of these transition energies and using a multivalley description of the impurity wave function in an effective-mass approach, they could propose a symmetry to each recombination line they observed. In particular, they speculated that the DX center could be the donor level corresponding to a donor-acceptor pair recombination with electron wave function being a fully symmetric combination of the four equivalent L -conduction minima. Previous experimental examinations of the optical properties of alloy samples which contained some silicon impurities presented in the papers of Roach *et al.*⁵ have revealed complicated temperature and energy dependences of the photoluminescence spectra with the hydrostatic pressure. Pressure-induced modifications of expected interlevel couplings prevented these authors from giving any clear determination of the contribution of all conduction-band extrema to the pressure coefficient of a given level, especially near the direct-indirect crossover. They suggested identifying the lower-energy component of their luminescence band (labeled B in their paper) with the D_4A transition identified as DX by Henning, Ansems, and Roksnoer.⁴ This level was experiencing a blueshift up to 4 GPa, then a redshift for higher pressure. Reevaluation of these data using an elementary calcula-

tion of the influence of the pressure on the different levels of the donor in $\text{Ga}_{0.7}\text{Al}_{0.3}\text{As}$ suggests that we label this transition D_3A instead of D_4A . The nonlinear dependence of the level under hydrostatic pressure is found to result in L - X coupling by the donor potential. These authors did not observe any coupling of the Γ - X type which could only occur for an X -type donor wave function built by fully symmetric combination of the three equivalent X valleys, i.e., having A_1 symmetry. This is only possible for a group-VI substitutional donor, according to group theory.⁶ A recent examination of the pressure dependence of the DX level by deep-level transient spectroscopy (DLTS) in $(\text{GaAl})\text{As:Te}$ has suggested a mixed character (between L and X) to the pressure coefficient of this transition.⁷ Although this latter result is consistent with an effective-mass description, the results of these two hydrostatic pressure experiments do not allow us to reject Chadi and Chang's model,³ which treats the DX center as a deep trap. However, Chadi's model is rejected by Bourgoin, Feng, and Von Bardeleben⁸ who concluded in an effective-mass state after studies of electron-emission and -capture variations with the alloy composition.

In this paper, we study the photoluminescence band of $\text{Ga}_{0.7}\text{Al}_{0.3}\text{As:Si}$ by using piezomodulation spectroscopy and show the applicability of an effective-mass description of the symmetry of all photoluminescence lines. Piezomodulation spectroscopy is a powerful *differential* method which enables us to elucidate a large number of band-structure problems in bulk⁹ semiconductors and is now successfully applied to low-dimension systems such as quantum wells and superlattices.^{10,11} In contrast to high-pressure studies the modification of the whole energy spectrum is small and the previously discussed pressure-induced modifications of interlevel couplings can be ignored with an extremely good approximation, due to the small deformations involved in this perturbation. To analyze results provided by this investigation, an additional experiment is required in order to obtain the first derivative of the unperturbed photoluminescence spectrum: a wavelength modulation of the photoluminescence spectrum.¹⁰ Basic principles of the method are given in Sec. II of the present paper. Comparing data ob-

tained by these two experiments, we could give an assignment to each recombination line of the complex luminescence band of our sample. The modulation ratio of all transitions has been interpreted in terms of expansion of the donor wave function along the various minima of the first conduction band. A pressure dependence of 5.8 ± 0.5 meV/kbar could be estimated for the level D_4A lower-energy zero-phonon transition. Because this transition exactly follows the L band in the alloy, we suggest this value be considered as a measurement of the pressure coefficient of the L band in (Ga,Al)As.

II. EXPERIMENT

The sample has been grown by MBE (molecular-beam epitaxy); it consists of a GaAs semi-insulating substrate on which a 1- μm nonintentionally doped (GaAl)As buffer layer has been grown before 3 μm of silicon-doped (Ga,Al)As were deposited with a Si dopant density of $9 \times 10^{17} \text{ cm}^{-3}$. The growth temperature was 610°C. Photoluminescence data presented in this section were taken at 2 K and at ~ 25 K (when the sample and the piezoelectric transducer attached to a cold finger were cooled by conduction) with a 50-cm focal length Jobin-Yvon HRS spectrometer, using the 514.5-nm green radiation of an ionized argon laser and with several red radiations of a cw dye laser loaded with 2-2-4 dimethyl-amino-propane dinitril (DCM).

Figure 1 summarizes spectroscopic data taken at 2 K. A measurements of the reflectivity at 2 K [spectrum 1(a)] gives us an idea of the direct band gap of the epilayer. The onset of the low-energy oscillations, which vanish when the semiconductor starts to absorb the light, occurs above 1934–1937 meV. Using the aluminum mole fraction (x) band-gap law recently published by Bosio *et al.*¹² and a Rydberg energy of 5 meV gives approximately an aluminum concentration of 30% in the sample. Photoreflectance spectroscopy measurement [Fig. 1(b)] has been done in order to cancel the interference system. We observe one differential structure at the energy of the band gap obtained by standard reflectivity. The photoluminescence occurs at low energy [see Fig. 1(c)]. A strong maximum at 1896 meV is observed when the green line of argon is used [Fig. 1(c)]. Increasing the sensitivity of the detection enables the observation of the emergence of transitions at 1780 and 1747 meV [as an illustration, the 1780-meV transition is plotted in Fig. 1(d)]. These transitions are hardly resolved in the low-energy wing of the photoluminescence band. Photoluminescence excitation (PLE) spectroscopy data (the dotted line in Fig. 1(c)) confirm the value of the band-gap energy obtained from the reflectance and photoreflectance experiments.

Increasing the temperature of the experiment up to 25 K, the 2-K photoluminescence band becomes structured. The shape of the whole photoluminescence is also a complicated function of the pump energy [see Figs. 2(b)–2(d)]. This witnesses the complicated mechanisms ruling the relative amplitudes of the photoluminescence structures in the sample. The best experimental resolution has been observed when setting the energy of the

pump laser at the excitonic energy obtained from the reflectivity experiment [spectrum (c) in Fig. 2]. The piezomodulation experiment was performed in these temperature and excitation conditions. Table I summarizes the full series of energies characteristic of this sample.

Spectra in piezomodulation and wavelength-modulation spectroscopy were also taken at ~ 25 K. To obtain the wavelength-modulation spectrum, the emitted wavelength is modulated inside the monochromator by replacing the mirror before the exit slit with a mirror which can be made to oscillate at a frequency of some hundred hertz with a lead-titanate-zirconate piezoelectric transducer. The intensity of the diffracted light slightly varies around its mean value at the oscillating frequency of the transducer. Setting the reference frequency of a lock-in amplifier at this frequency, one observes a signal closely proportional to the first energy derivative of the unmodulated spectrum. In the piezomodulation experiment the physical properties of the sample are modulated in the following way: the sample is attached to cylindrical piezoelectrical transducer submitted to an alternating voltage of roughly 350 V. The breathing modes of the

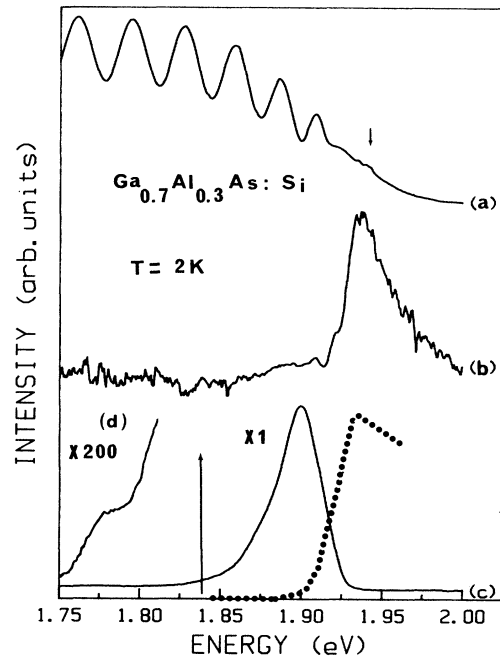


FIG. 1. (a) Reflectivity spectrum taken at 2 K for $\text{Ga}_{0.7}\text{Al}_{0.3}\text{As}$ grown on GaAs. Note the series of interferences in the alloy epilayer. The onset of absorption at the band-gap energy cancels this interference system. (b) Photoreflectance spectrum of the sample. The interferences have been quenched and a derivative structure is observed at the energy of the band gap. (c) Photoluminescence (solid line) and photoluminescence excitation (dotted line) data. Note the Stokes shift between the spectra; the onset in the PLE (which was taken by setting the monochromator at the energy of the arrow) corresponds to the energy of the band gap deduced from reflectance and photoreflectance spectroscopy. (d) Low-energy wing of the 2-K PL spectrum displayed in (c).

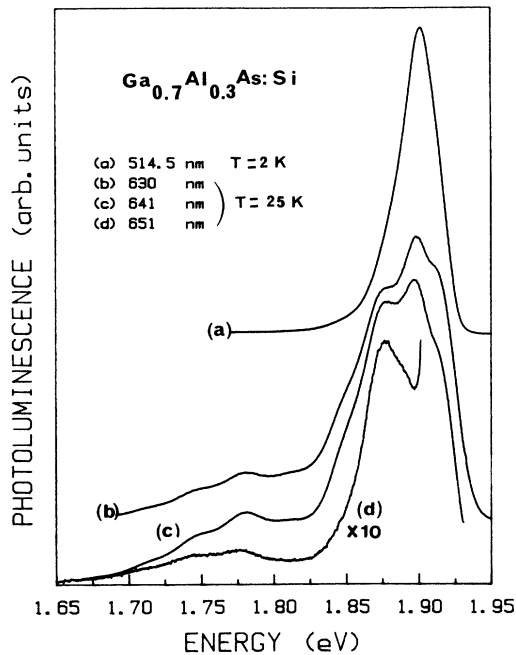


FIG. 2. Change of the photoluminescence spectrum with the temperature (compare *a* with *b*, *c*, and *d*). The spectra become structured when the temperature is increased. The efficiency of the PL also depends on the absorption coefficient at the wavelength of the pump laser. These behaviors are used in order to select the experimental conditions for performing the piezomodulation spectroscopy experiment.

transducer produce alternating planar expansions and contractions of the sample. To such periodic strain fields correspond periodic modifications of the band structure. The amplitudes of these variations are a function of the deformation potentials of each relevant point of the first Brillouin zone. Setting the frequency of the lock-in amplifier to the modulation frequency, one easily detects energy-oscillating transitions while energy-stationary transitions are silent. The modulation efficiency for a given transition is then *directly* obtained by division of the intensity of each structure of the piezomodulated spectrum with the corresponding intensity of the wavelength-modulated spectrum.

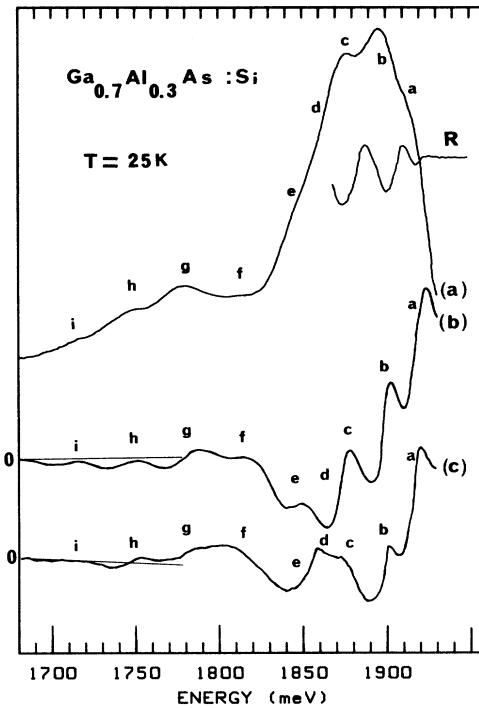


FIG. 3. (a) Photoluminescence; (b) wavelength modulation of the photoluminescence; (c) piezomodulation of the photoluminescence and reflectance (*R*). Spectra *a*, *b*, and *c* were taken at 25 K using a 641-nm radiation for the pump laser.

The corresponding results are gathered in Fig. 3. The photoluminescence data have been included [Fig. 3(a)] as well as a reflectance spectrum (*R*). Figure 3(b) displays the wavelength modulation of the direct luminescence spectrum of Fig. 3(a). The labeling is common to Table I and the figures. Differential structures corresponding to energy levels labeled *a* and *c* exhibit a common behavior under coplanar stress (the amplitudes of the wavelength-modulated and piezomodulated structures are in the same ratio). We suggest identifying them by a zero-phonon transition *a* together with one phonon-replica *c* ($\hbar\omega_{\text{ph}} = 34.54$ meV). The same trend is observed at low energy: levels *f*, *g*, *h*, and *i* behave similarly within the

TABLE I. Transition energies measured at 5 K.

Energy (meV)	Character	Identification	Label
1910.42	Γ	$D_1 - A$	<i>a</i>
1896.03	L, X	$D_3 - A$	<i>b</i>
1875.88	Γ	$D_1 - A - \text{LO}_{\text{GaAs}}$	<i>c</i>
1862 ^a	Γ	$D_1 - A - \text{LO}_{\text{AlAs}}$	<i>d</i>
1848.53	L, X	$D_3 - A - \text{LO}_{\text{AlAs}}$	<i>e</i>
1812.55	L	$D_4^0 h$	<i>f</i>
1779.45	L	$D_4 - A$	<i>g</i>
1746.35	L	$D_4 - A - \text{TO}_{\text{GaAs}}$	<i>h</i>
1713.25	L	$D_4 - A - 2\text{TO}_{\text{GaAs}}$	<i>i</i>

^aResolved in piezomodulation only.

experimental uncertainty. The energy of structure g corresponds to the energy expected for the transition labeled $D_4 A$ in the paper of Henning, Ansem, and Roksnoer.⁴ A deconvolution of the intensity of these transitions has shown that the intensities of levels g to i obey a Huang-Rhys law. The replicas involve a phonon energy of 33.1 meV, a value smaller than the 48-meV value given in Ref. 4. The Huang-Rhys factor is also different: i.e., 0.8 instead of 0.5. However, both fittings give nearly the same value for the relaxation energy: 25 meV. Actually, a plausible identification is to consider that h and i are phonon replicas of g ($\hbar\omega_{\text{ph}}=33.10$ meV) and that f is a $D_4^0 h$ transition. Another possibility is to consider f as a zero-phonon line and g as a replica of f . In this case, a Huang-Rhys factor of 1.3 is deduced.

We now compare the intensity of structure a in the two experiments: its signature is plotted larger in piezomodulation than in wavelength modulation. Low-energy structures f to i appear weaker in the piezomodulation spectrum than in the wavelength-modulation data. Taking the identity for modulation efficiency of structure a [i.e., scaling the amplitude of spectrum 3(b) in such a way to deal with identical wavelength-modulated and piezomodulated features for structure a], structure g has a modulation efficiency of 0.464 ± 0.009 . We also measure a modulation efficiency of 0.46 ± 0.02 for structure b and e . We propose to identify structure d , detected in piezomodulation only, with a second kind of phonon replica of a ($\hbar\omega_{\text{ph}} \sim 48$ meV).

We now discuss this series of phonon energies in light of Raman-scattering investigations made by Jusserand and Sapriel.¹³ The long-wavelength optical phonons of (Ga,Al)As display a two-mode behavior. In our present case, where the aluminum concentration is ~ 0.3 and using the frequency variations with the aluminum concentration given in Fig. 1 of Ref. 13, we estimate the following phonon energies: $E_{\text{LO}_{\text{GaAs-like}}} = 35$ meV, $E_{\text{TO}_{\text{GaAs-like}}} = 33$ meV, $E_{\text{LO}_{\text{AlAs-like}}} = 47$ meV, and $E_{\text{TO}_{\text{AlAs-like}}} = 44$ meV. Comparison of these values together with the spectroscopy data will allow us to propose the identification of all transition energies given in Table I.

III. DATA ANALYSIS

In the multivalley description of the donor wave function, expansions along linear combinations of the conduction-band minima having A_1 and T_2 symmetry occur. Let

$$\begin{aligned} X &= (2\pi/a)(1, 0, 0); \quad Y = (2\pi/a)(0, 1, 0); \\ Z &= (2\pi/a)(0, 0, 1); \quad L_1 = (\pi/2a)(1, 1, 1); \\ L_2 &= (\pi/2a)(1, -1, -1); \quad L_3 = (\pi/2a)(-1, 1, -1); \\ L_4 &= (\pi/2a)(-1, -1, 1) \end{aligned}$$

be the labeling of the satellites conduction-band minima (Camel's back effect is neglected). Then combinations having A_1 symmetry are

$$A_1^\Gamma = \Gamma$$

and

$$A_1^L = (L_1 + L_2 + L_3 + L_4)/2.$$

Combinations having the threefold T_2 symmetry are written $[X, Y, Z]$ and $[(L_1 + L_2 - L_3 - L_4)/2, (L_1 - L_2 + L_3 - L_4)/2, (L_1 - L_2 - L_3 + L_4)/2]$. Following the treatment of impurity states in multivalley semiconductors,¹⁴ the electronic spectrum is obtained by calculating the eigenvalues of a 4×4 matrix of the kind

$$\begin{pmatrix} A_1^\Gamma \rangle & A_1^L \rangle & T_2^x \rangle & T_2^{Lx} \rangle \\ \left[\begin{array}{cccc} H_1^\Gamma & \Delta_{\Gamma L} & 0 & 0 \\ & H_1^L & 0 & 0 \\ & & H_2^x & \Delta_{XL} \\ & & & H_2^{Lx} \end{array} \right] , \end{pmatrix}$$

where the off-diagonal matrix elements of the impurity potential are noted Δ_{ij} and the self-energies H_i^j . Including the influence of the external stress from the piezomodulation on the conduction states provokes the following splitting of the T_2^x and T_2^L triplets:

$$\begin{pmatrix} T_2^{y,x} \rangle & T_2^{L,y,x} \rangle & T_2^z \rangle & T_2^{Lz} \rangle \\ \left[\begin{array}{cccc} H_2^x & \Delta_{XL} & 0 & 0 \\ & H_2^{Lx} & 0 & 0 \\ & & H_2^z & \Delta_{XL} \\ & & & H_2^{Lz} \end{array} \right] . \end{pmatrix}$$

The diagonal elements are given by

$$\begin{aligned} H_1^\Gamma &= E^\Gamma - D^{0\Gamma} + 2a_c S^+, \\ H_1^L &= E^L - D^{0L} + 2E_1' S^+ - 3\nu, \\ H_2^x &= E^x - D^{0x} + 2E_1 S^+ + E_2 S^- / 3, \\ H_2^z &= E^x - D^{0x} + 2E_1 S^+ - 2E_2 S^- / 3, \\ H_2^{Lx} &= H_2^{Lz} = E^L - D^{0L} + 2E_1' S^+ + \nu, \end{aligned}$$

where E^α is the energy position of the conduction minima α ; $D^{0\alpha}$ is the ionization of the donor level pinned to this minima; ν is the L - L valley-orbit interaction parameter. $S^+ = (S_{11} + 2S_{12})\sigma$ and $S^- = (S_{11} - S_{12})\sigma$ are the combinations of the elastic constants of the epilayer times the biaxial stress σ . E_1 , E_1' , and a_c are the hydrostatic deformation potentials of the X , L , and Γ minima, respectively; E_2 is the tetragonal shear-deformation potential of the X conduction band. The movement of all electronic levels under the coplanar stress can be obtained analytically as a function of all the parameters above.

The experimental energies correspond to differences between electronic and acceptor energies; the influence of the coplanar stress on the acceptor state has to be expressed. The acceptor problem under coplanar stress has been treated by Freundlich, Neu, and Grenet¹⁵ using the suitable envelope functions given by Baldereschi and Lipari¹⁶ and also including the interaction between the acceptor ground state and its excited state under stress.¹⁷ The acceptor-state splitting δ_A of the $m_j = \pm \frac{1}{2}$ and $m_j = \pm \frac{3}{2}$ acceptor components is

$$\delta_A = b(1 - 4\mu^2/5)S^-,$$

where b is the valence-band tetragonal shear-deformation potential and μ is a function of the Luttinger parameters,

$$\mu = (6\gamma_3 - 4\gamma_2)/5\gamma_1.$$

The shifts of the effective-mass acceptor components are given by

$$\delta E_{A\pm 1/2} = 2a_v S^+ - \delta_A,$$

where a_v is the valence-band hydrostatic deformation potential. E^Γ , E^x , and E^L are functions of the aluminum concentration x ,

$$E^\Gamma = 1519 + 1360x + 220x^2 \text{ (meV)}$$

(see Ref. 12),

$$E^x = E^x(\text{GaAs}) + 125x + 143x^2 \text{ (meV)}$$

(see Ref. 18), and

$$E^L = E^L(\text{GaAs}) + 642x \text{ (meV)}$$

(see Ref. 18), with $E^x(\text{GaAs}) = E^\Gamma(\text{GaAs}) + 485 \pm 10$ meV and $E^L(\text{GaAs}) = E^\Gamma(\text{GaAs}) + 310 \pm 10$ meV.¹⁹⁻²¹ The choice of these composition-dependence laws has a non-negligible influence on the values of donor ionization energy and coupling parameters which are fitting parameters but will not affect the modulation ratio which mainly depends on the interlevel splittings. Values of the donor ionization energies $D^{0\Gamma}$, D^{0x} , and D^{0L} fitted by Henning, Ansems, and Roksnoer⁴ using other composition-dependence laws were 7, 70, and 122 meV, respectively. The intervalley parameter $\Delta_{\Gamma L}$ cannot be measured in this sample when the aluminum concentration is so important, due to the large splitting between E^Γ and E^L and the consequent energy difference between line a and line g . Henning, Ansems, and Roksnoer⁴ measured 12.5 meV for Δ_{XL} from composition-dependence studies of the transition energies. A reevaluation of the data of Henning, Ansems, and Roksnoer enables us to estimate $\nu = 30$ meV; then using our spectroscopical data together with $D^{0\Gamma} = 7$ meV (Ref. 20) and $D^{0x} = 70$ meV (Ref. 22) we get $D^{0L} \sim 118$ meV and $\Delta_{XL} = 12.5$ meV. These values differ slightly from the data given in Ref. 4, except Δ_{XL} . They have been obtained using an aluminum composition of 0.305 (such an accuracy is required by the calculation) and taking a free-exciton Rydberg of 5 meV. We calculate $D_1 A = 1905$ meV, $D_2 A = 1953$ meV, $D_3 A = 1898$ meV, and $D_4 A = 1780$ meV, a series to be compared with the energies of Table I. A calculation of the transition energies using the proposal of Henning, Ansems, and Roksnoer and $\nu = 32$ meV and $D^{0L} = 122$ meV gives comparable results but requires $x = 0.325$ to properly locate the energy position of the $D_1 A$ transition. This illustrates the accuracy and the limits of the model.

In GaAs, values of -9 and -0.4 eV have been proposed for the hydrostatic deformation potentials of the zone-center conduction and valence-band deformation potential,²³ respectively. The pressure dependence of the direct band gap of $\text{Ga}_{0.7}\text{Al}_{0.3}\text{As}$ is equal to 9.9

meV/kbar;²⁴ using a scaling argument we deduce $a_c = -8.25$ eV and $a_v = -0.37$ eV in the alloy. From earlier measurements of the pressure-induced redshift of the (Ga,Al)As indirect Γ - X band gap (~ -1.34 meV/kbar),^{25,26} we deduce $E_1 = 0.7$ eV; a linear interpolation between the GaAs (Ref. 21) and AlAs (Ref. 27) values of E_2 gives $E_2 = 6.5 - 1.4x$. The deformation potential E'_1 is not known accurately due to a large scattering in the literature.²⁸ A value will be proposed at the end of this section. For b , we take the GaAs data published by Chandrasekhar and Pollak:²⁹ -1.76 eV.

To go further, we can calculate the biaxial stress dependence of all conduction levels for various values of E'_1 . Similar calculations can also be made for the acceptor level *mutadis mutandis*. The important point to outline at this stage concerns the magnitude of the level shifting provoked in case of the biaxial stress: due to the magnitude of σ (~ 0.01 kbar), the energy shifts are always small compared to the width of the transitions; as a consequence, although the stress lifts the degeneracy of the acceptor level, such splitting cannot be resolved experimentally. We measure a contribution of all levels weighted by a coefficient depending on the experimental conditions. In the present case, where the propagation of the incident photon occurs perpendicular to the plane of the applied stress, i.e., for σ polarization, the contributions of the $m_{3/2}$ and $m_{1/2}$ components of the acceptor are in a ratio of 3-1. Then, the acceptor contribution to the energy shift is given by

$$\delta E_A = \frac{1}{4}\delta E_{A\pm 1/2} + \frac{3}{4}\delta E_{A\pm 3/2}.$$

A similar effect also occurs for T_2 levels but X like, Y like, and Z like have the same weight, the shear effects cancel for T_2^x, y and T_2^z , and we deal with the resulting contribution.

The stress dependence of the $D_1 A$ level equals 5.12 meV/kbar; then a ratio of 0.476 ± 0.009 between the slope of $D_4 A$ and the slope of $D_1 A$ can be obtained fitting E'_1 to -4.99 ± 0.07 eV. In terms of the widening of the band gap under hydrostatic pressure conditions, this means 5.8 ± 0.1 meV/kbar in the range of values quoted in the literature for GaAs.^{19,21} Under biaxial stress, transition $D_3 A$ exhibits a slope of 2.21 meV/kbar while transition $D_2 A$ should shift at a rate of -1.72 meV/kbar. Modulation efficiencies of 0.43 and -0.336 are expected for these transitions. The modulation efficiency observed for $D_3 A$ was 0.46, in close agreement with the calculated value. The $D_2 A$ level is not observed, because the D_2 level of the donor is resonant in the Γ conduction band. The biaxial stress dependence of the photoluminescence band of $\text{Ga}_{0.7}\text{Al}_{0.3}\text{As}$ can be accurately described by using an effective-mass description of the donor wave function.

We finally have calculated the modification of the fan of these effective-mass electronic levels when $\text{Ga}_{0.7}\text{Al}_{0.3}\text{As}$ is submitted to hydrostatic pressure. We have ignored the influence of the pressure on the valley-orbit interactions. We find $D_3 A$ which is calculated to behave strongly nonlinearly under hydrostatic pressure to be a good candidate for the transition labeled D in Ref. 5

rather than $D_4 A$ which behaves quasilinearly under pressure. The origin of the transitions labeled B and C in the same paper are still mysterious; the possibility that they correspond to another impurity cannot be ruled out.

IV. CONCLUSION

We have studied the photoluminescence and reflectance properties of $\text{Ga}_{0.7}\text{Al}_{0.3}\text{Si}$ by means of piezomodulation, wavelength-modulation, and photomodulation spectroscopy. We could identify the luminescence lines by their comparative behavior under piezomodulation and wavelength modulation of the photoluminescence. The fan of energy levels observed could be

accounted for with a multivalley expansion of the donor wave function along the minima of the lowest conduction band. Within this model, a value is proposed for the $\Gamma_8^v-L_6^c$ hydrostatic deformation potential E_1' : -4.99 ± 0.07 eV.

ACKNOWLEDGMENTS

This work is supported by a European Economic Community (EEC) Contract "Esprit Basic Research No. 3168." The authors would like to express their thanks to Dr. J. Allegre, Dr. G. Neu, and Dr. P. Gibart for fruitful discussions and J. C. Portal and J. M. Salles for magnetotransport measurements on the sample.

*Permanent address: Groupe d'Etudes des Semiconducteurs, Université de Montpellier II: Sciences et Techniques du Languedoc, Case Courrier 074, place Eugène Bataillon, 34095 Montpellier CEDEX 05, France.

†Permanent address: ISA RIBER, 133-137 Boulevard National, Boîte Postale 231, 92503 Rueil-Malmaison, France.

¹See, for instance, D. V. Lang, in *Deep Centres in Semiconductors*, edited by S. T. Pantelides (Gordon and Breach, New York, 1985); *Physics of DX Centers in GaAs Alloys*, edited by J. C. Bourgoin (Scientific Technological Publications, 1986); P. M. Mooney, *J. Appl. Phys.* **67**, R1 (1990).

²T. N. Theis, in *Proceedings of the 3rd International Conference on Shallow Impurities in Semiconductors, Linköping, Sweden, 1988*; edited by Bo Monemar, IOP Conf. Proc. No. 95 (Institute of Physics and Physical Society, London, 1990), p. 307.; D. Lavielle, B. Goutiers, A. Kadri, E. Ranz, L. Dmowski, J. C. Portal, C. Grattapain, N. Chand, J. M. Sallesse, and P. Gibart, in *Proceedings of the 20th International Conference on the Physics of Semiconductors, Thessaloniki, 1990*, edited by E. M. Anastassakis and J. D. Joannopoulos (World Scientific, Singapore, 1991), p. 521; A. Kadri, E. Ranz, K. Zitouni, N. Saidi, J. C. Portal, D. Lavielle, R. Sirvin, C. Grattapain, and N. Chand, *Proceedings of the 4th International Conference on High Pressure in Semiconductor Physics, Porto Carras, Greece, 1990* [Semicond. Sci. and Technol. (to be published)].

³T. N. Morgan, *Phys. Rev. B* **34**, 2664 (1986); H. Hasegawa and H. Ohno, *Jpn. J. Appl. Phys.* **25**, L319 (1985); J. D. Chadi and K. J. Chang, *Phys. Rev. Lett.* **61**, 873 (1988); *Phys. Rev. B* **39**, 10063 (1983); H. P. Hjalmarson and T. J. Drummond, *Appl. Phys. Lett.* **48**, 656 (1986); J. C. Bourgoin and A. Mauger, *ibid.* **53**, 749 (1988).

⁴J. C. M. Henning, J. P. M. Ansems, and P. J. Roksnoer, *Semicond. Sci. Technol.* **3**, 361 (1988).

⁵W. P. Roach, M. Chandrasekhar, H. R. Chandrasekhar, F. A. Chambers, and J. M. Meese, *Semicond. Sci. Technol.* **4**, 290 (1989).

⁶T. N. Morgan, *Phys. Rev. Lett.* **21**, 819 (1968).

⁷W. Shan, P. Y. Yu, M. F. Li, W. L. Hansen, and E. Bauser, *Phys. Rev. B* **40**, 7831 (1989).

⁸J. C. Bourgoin, S. L. Feng, and H. J. von Bardeleben, *Phys. Rev. B* **40**, 7663 (1989).

⁹P. Merle, D. Auvergne, and H. Mathieu, *Solid State Commun.* **19**, 771 (1976) and references therein.

¹⁰H. Mathieu, P. Lefebvre, J. Allegre, B. Gil, and A. Regreny, *Phys. Rev. B* **36**, 6581 (1987).

¹¹H. Mathieu, J. Allegre, and B. Gil, *Phys. Rev. B* **43**, 2218 (1991).

¹²C. Bosio, J. L. Staehli, M. Guzzi, G. Burri, and R. A. Logan, *Phys. Rev. B* **38**, 3263 (1988).

¹³B. Jusserand and J. Sapriel, *Phys. Rev. B* **24**, 7194 (1981).

¹⁴F. Bassani, G. Iadonisi, and B. Preziosi, *Rep. Prog. Phys.* **37**, 1099 (1974).

¹⁵A. Freundlich, G. Neu, and J. C. Grenet, *Solid State Commun.* **76**, 87 (1990).

¹⁶A. Baldereschi and N. O. Lipari, *Phys. Rev. B* **8**, 2697 (1973); **9**, 1525 (1974).

¹⁷M. Schmidt, *Phys. Status Solidi B* **79**, 533 (1977).

¹⁸S. Adachi, *J. Appl. Phys.* **58**, R1 (1985).

¹⁹D. E. Aspnes, *Phys. Rev. B* **14**, 5331 (1976).

²⁰D. J. Wolford and J. A. Bradley, *Solid State Commun.* **53**, 1059 (1985).

²¹D. N. Mirkin, V. F. Sapega, I. Ia. Karlik, and R. Katilius, *Solid State Commun.* **61**, 799 (1987).

²²M. Leroux (unpublished).

²³N. D. Nolte, W. Walukiewicz, and E. E. Haller, *Phys. Rev. Lett.* **59**, 501 (1987).

²⁴M. Chandrasekhar, U. Venkateswaran, H. R. Chandrasekhar, B. A. Vojak, F. A. Chambers, and M. J. Meese, in *Proceedings of the XVIIth International Conference on the Physics of Semiconductors, Stockholm, 1986*, edited by O. Engstrom (World Scientific, Singapore, 1987), p. 943.

²⁵See Fig. 5 of D. J. Wolford, T. F. Kuech, J. A. Bradley, M. A. Gell, D. Ninno, and M. Jaros, *J. Vac. Sci. Technol. B* **4**, 1043 (1986).

²⁶U. Venkateswaran, M. Chandrasekhar, H. R. Chandrasekhar, B. A. Vojak, F. A. Chambers, and J. M. Meese, *Phys. Rev. B* **33**, 8416 (1986).

²⁷P. Lefebvre, B. Gil, H. Mathieu, and R. Planel, *Phys. Rev. B* **40**, 7802 (1989).

²⁸This scattering is illustrated in Fig. 1 of Ref. 5.

²⁹M. Chandrasekhar and F. H. Pollak, *Phys. Rev. B* **15**, 2127 (1977).